UV SEDs of early-type cluster galaxies: a new look at the UV upturn

S. S. Ali,[1][*] M. N. Bremer,[1][*] S. Phillipps[1] and R. De Propris[2]

[1]*H.H. Wills Physics Laboratory, University of Bristol, Tyndall Avenue, Bristol BS8 1TL, UK*
[2]*FINCA, University of Turku, Väisäläntie 20, Piikkiö FI-21500, Finland*

ABSTRACT

Using *GALEX*, Ultraviolet Optical Telescope (UVOT), and optical photometry, we explore the prevalence and strength of the Ultraviolet (UV) upturn in the spectra of quiescent early-type galaxies in several nearby clusters. Even for galaxies with completely passive optical colours, there is a large spread in vacuum UV colour consistent with almost all having some UV upturn component. Combining *GALEX* and UVOT data below 3000 Å, we generate for the first time comparatively detailed UV spectral energy distributions for Coma cluster galaxies. Fitting the UV upturn component with a blackbody, 26 of these show a range of characteristic temperatures (10 000–21 000K) for the UV upturn population. Assuming a single temperature to explain *GALEX*-optical colours could underestimate the fraction of galaxies with UV upturns and mis-classify some as systems with residual star formation. The UV upturn phenomenon is not an exclusive feature found only in giant galaxies; we identify galaxies with similar (or even bluer) $FUV - V$ colours to the giants with upturns over a range of fainter luminosities. The temperature and strength of the UV upturn are correlated with galaxy mass. Under the plausible hypothesis that the sources of the UV upturn are blue horizontal branch stars, the most likely mechanism for this is the presence of a substantial (between 4 per cent and 20 per cent) Helium-rich ($Y > 0.3$) population of stars in these galaxies, potentially formed at $z \sim 4$ and certainly at $z > 2$; this plausibly sets a lower limit of $\sim 0.3 - 0.8 \times 10^{10}\,\mathrm{M_\odot}$ to the *in situ* stellar mass of $\sim L^*$ galaxies at this redshift.

Key words: stars: horizontal branch – galaxies: clusters: individual: Coma – galaxies: evolution – galaxies: formation.

1 INTRODUCTION

Despite their generally old and metal-rich stellar populations, massive early-type galaxies often show excess flux at $\lambda < 3000$ Å above what is expected from conventional stellar evolution (Code 1969; Bertola, Capaccioli & Oke 1982). It is now generally accepted that the UV excess (hereafter upturn) originates from hot horizontal branch (HB) stars (e.g. see review by O'Connell 1999; Yi 2008). Two general conditions must apply to this upturn population. First, any hot HB population giving rise to an upturn in a massive early-type galaxy cannot be metal-poor because the broad-band colours and line indices of early-type galaxies (e.g. Burstein et al. 1988; Pastorello et al. 2014) clearly show that they are dominated by a metal-rich stellar population. Secondly, as HB stars represent the late core Helium burning phase of low-mass stars, the upturn directly probes the properties of stars that reached the zero age main

sequence at relatively high redshift and therefore provides a window to the conditions within galaxies at very early times.

The upturn, as measured by the $FUV - V$ colour, appears to be correlated with metallicity (more properly, Mg$_2$ strength) and velocity dispersion, in the sense that more massive and metal-rich galaxies have bluer UV-optical colours (Burstein et al. 1988; Bureau et al. 2011). However, it shows very weak correlation with the Iron-abundance indices (Fe5015), suggesting that the source of the upturn is related to the α-enriched older stellar populations (O'Connell 1999; Bureau et al. 2011). Boselli et al. (2005) extended the earlier work by performing a cluster-wide survey for the upturn in all early-type galaxies in the Virgo cluster, going all the way down to dwarf ellipticals. They recovered the correlations between $FUV - V$ and metallicity as with Burstein et al. (1988) in the brightest galaxies; however, this correlation did not necessarily hold true for the fainter galaxies. Even though the upturn tended to get stronger with increasing mass (or luminosity) in giant ellipticals, they found that the opposite was true for dwarf ellipticals. Smith, Lucey & Carter (2012) recovered a similar result when looking at a large sample of optically selected giant early-type galaxies in

*E-mail: s.ali@bristol.ac.uk (SSA); m.bremer@bristol.ac.uk (MNB)

the Coma cluster and found a reddening in the *FUV − i* colour as the galaxy luminosity decreased (i.e. mass decreased). Schombert (2016) also carried out multicolour photometry for a large sample of local ellipticals using a combination of *GALEX*, Sloan Digital Sky Survey (SDSS), 2-Micron All-Sky Survey (2MASS), and *Spitzer* data. He found that the *NUV*-optical colours in particular were a direct measure of the UV upturn and changed with galaxy luminosity. These colours could only be reproduced by using models with a range of blue HB populations.

One promising mechanism that produces a UV upturn is having a Helium-enriched population of stars on the HB. While an increase in metallicity generally decreases the temperature of a stellar population due to increasing opacity in the stellar envelope, if the Helium abundance is sufficiently high, it acts to decrease the opacity such that the measured surface temperature of the star increases. In particular, for HB stars where the envelope is already significantly thinned, this can cause a substantial rise in the measured surface temperature of the stars compared to those with more normal Helium abundances. This allows the possibility that even in systems that have high metallicity, a significant (metal-rich) blue HB component can exist, clearly important in explaining UV upturns in early-type galaxies (Norris 2004; Lee et al. 2005a; Chung, Yoon & Lee 2017, see also review by O'Connell 1999).

Besides Helium-enriched blue HB stars being a potential origin of the upturn, other models have also been proposed to explain this phenomenon, in particular with enhanced mass-loss in metal-rich stars [where these stars lose more mass as they ascend the red giant branch (RGB) – Yi, Demarque & Oemler 1997] and the binary evolution model (similar to the hot sub-dwarfs in our Galaxy – Han, Podsiadlowski & Lynas-Gray 2007). However, neither of these mechanisms has observational support (see Section 4) and would not account for observations in local open and globular clusters.

In this paper, we expand upon the work of Boselli et al. (2005) and Smith et al. (2012). The approach we take is as follows: we construct the most detailed UV spectral energy distribution (SED) possible from the available photometry for red sequence galaxies drawn from the Coma cluster, combining each with their optical SED. We then fit the entire SED with a combination of a conventional old stellar population and a blackbody. The conventional stellar population does not include a UV-luminous post-main sequence population with which to explain the UV upturn; the additional blackbody is used to model and characterize this. The best-fitting temperature of this blackbody component could be interpreted as the luminosity-weighted temperature of any population that gives rise to the UV upturn. We also compare the *FUV* colours of the Coma galaxies with those of similar galaxies in the Fornax and Perseus clusters in order to analyse the strength of the upturn in all three. Lee et al. (2005b) carried out photometry of some of the brightest galaxies in the Fornax cluster; however, given the subsequent availability of much deeper *GALEX* data, we are able to detect a larger number of galaxies and present a more comprehensive study of this cluster.

In the following, all magnitudes quoted are in the AB system, and the cosmology used assumes $h = 0.7$, $\Omega_m = 0.3$, $\Omega_\Lambda = 0.7$. We correct for Galactic extinction for Perseus galaxies in all bands, using the extinction maps provided by Schlafly & Finkbeiner (2011). However, due to the large amount of extinction present particularly in the UV bands, and the possibility of there being slightly varying amounts of extinctions along different lines of sight, there is a small yet intrinsic uncertainty in the extinction-corrected UV photometry for the Perseus cluster.

2 DATA

2.1 Optical

Our main focus is on the Coma cluster, but we also carry out a comparison with the Fornax and Perseus clusters. We select the optical cluster red sequence, as this is known to host the majority of cluster members and to consist of mainly 'red and dead' E/S0 galaxies (Bower, Lucey & Ellis 1992). Data for Coma and Perseus are taken from the latest release (DR12) of the SDSS (York et al. 2000; Alam et al. 2015). We select only those red sequence members with uncertainties <0.05 mag in their relevant optical colours. We use a metric (7.5 kpc diameter) aperture to measure UV-optical colours. For Fornax, we use the *B* and *V* data from Karick, Drinkwater & Gregg (2003),[1] and for Coma and Perseus, we convert (where necessary) the SDSS *g* − and *r*-band magnitudes to equivalent *V* magnitude using the equations from Jester et al. (2005). Galaxies on the red sequence are assumed to be cluster members, as is usually the case, but we also use published catalogues to check membership [Coma: Michard & Andreon 2008; Hammer et al. 2010b and Trentham et al. (private communication); Fornax: Ferguson & Sandage 1988; Drinkwater et al. 2000; Perseus: Brunzendorf & Meusinger 1999]. We plot these red sequences in Fig. 1.

2.2 *GALEX*

The UV images for the Fornax, Perseus, and Coma clusters were obtained from archived Galaxy Evolution Explorer (*GALEX* – Martin et al. 2005; Morrissey et al. 2007) data, available through the Multi-Mission Archive at the Space Telescope Science Institute (MAST). Images were obtained for both *GALEX* filters: *FUV* and *NUV* that have central wavelengths 1526 Å (range of 1344–1786 Å) and 2329 Å (range of 1771–2831 Å) and image resolution FWHM of 4.3 and 5.3 arcsec, respectively.

All images were retrieved as calibrated intensity maps (plus their relative σ images) from the GalexView tool (https://galex.stsci.edu/galexview). Exposure times for Coma images were 19 and 30 ks in the *FUV* band (Hammer et al. 2010a). For Perseus, the exposure times in *FUV* were 14.9 and 8 ks (O'Connell et al. 2005), and for Fornax, we used a deep exposure of 34 ks in the centre and a 'ring' of 12 2.5 ks exposures in the outer regions (NGS – Nearby Galaxy Survey; Gil de Paz et al. 2007).

We measured *FUV* and *NUV* magnitudes for red sequence galaxies in these clusters through 7.5 kpc (diameter) apertures, centred on the optical position. We only consider objects with >5σ detections and verify their reality by eye. This process ensured that all red sequence Coma galaxies to 2 mag below M^* in the *H* band (Eisenhardt et al. 2007) were included in our sample.

2.3 Ultraviolet Optical Telescope

Ultraviolet Optical Telescope (UVOT) is an ancillary 30 cm telescope on the *SWIFT* satellite. It has a field of view of 17 arcmin × 17 arcmin with a pixel scale of 0.502 arcsec and a point spread function (PSF) full width at half-maximum (FWHM) of 2.5 arcsec. Technical descriptions of the *SWIFT* UVOT telescope and its photometric calibrations are given in Roming et al. (2005) and Poole et al. (2008). UVOT images for Coma were taken through the *UVW2* (central wavelength 1928 Å), *UVM2*(2246 Å), *UVW1* (2600 Å) filters, as well as optical filters. We only use the *UVW2* and *UVW1*

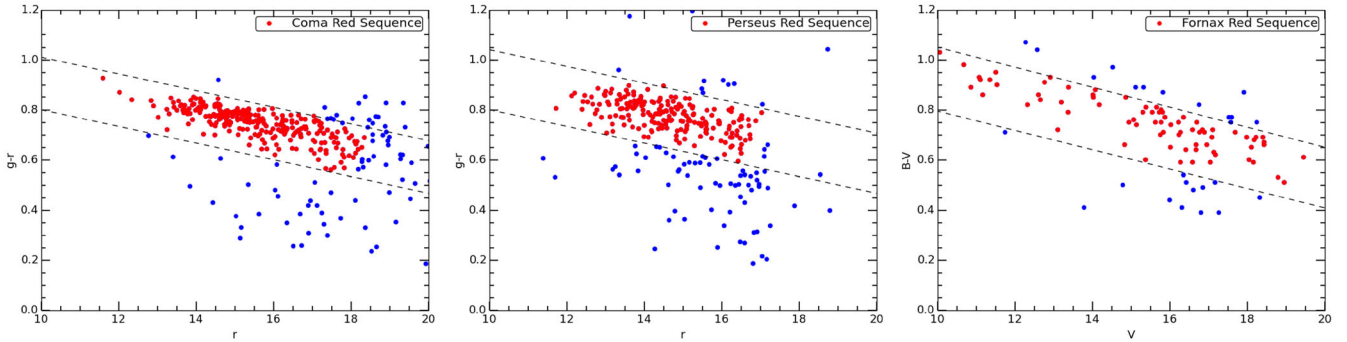[1] In this case, we use their Kron (model) apertures.

Figure 1. Optical colour–magnitude diagrams ($g − r$ or $B − V$ versus r or V) for the Coma, Perseus and Fornax clusters (left to right). The red sequence is denoted by the dashed lines in each case (medium gray in print version and red in online version; see online version of paper for colour plots). Galaxies used in this analysis are those red sequence objects with photometric uncertainties in their optical colour <0.05 mag. All colours are corrected for foreground extinction as described in the main text.
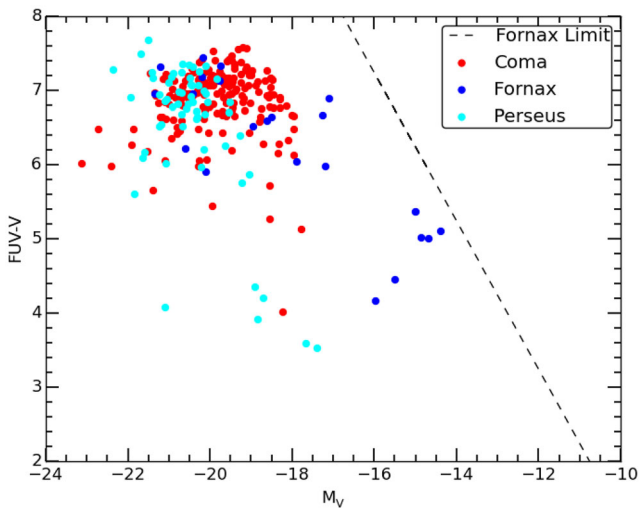

Figure 2. $FUV(GALEX) − V$ versus M_v colour–magnitude diagram for red sequence galaxies in Coma, Fornax, and Perseus clusters. The black dashed line shows the *GALEX FUV* detection limit ($>5\sigma$) for Fornax. Photometric error in colour is <0.1 mag.

data in conjunction with the optical *U*, *B*, and *V* UVOT images, given that the *UVM*2 band largely overlaps with the *GALEX NUV* band and has a far shorter total exposure time in comparison.

For Coma, we were able to find images in the *SWIFT* UVOT archive from multiple programmes (Markwardt et al. 2005; Brown et al. 2014). These covered a subset of the Coma galaxies observed with *GALEX* and depending upon the number and/or depth of individual exposures, resulted in a variety of effective exposure times. The deepest exposures came from overlapping pointings that targeted the centre of the cluster. Most of the UVOT-targeted galaxies ($\sim$24 out of 42) are drawn from this region and consequently have deeper ($\sim$2.7–3.4 ks in *UVW*2 and $\sim$0.8–1.3 ks in *UVW*1) exposure times. For the galaxies outside of this region, exposure varied between $\sim$0.8–2.7 ks in *UVW*2 and $\sim$0.15–0.8 ks in *UVW*1. Despite the variation in exposure times, all galaxies detected by *GALEX* and targeted by UVOT are detected. However, while the *GALEX* observations sampled passive galaxies down to $M_v = −18$ (Fig. 2), the UVOT pointings only targeted one galaxy fainter than $M_v > −19$.

The images were aligned and averaged together using the *imcombine* function in IRAF to create final images with longer exposure times to perform photometry on. Similar to *GALEX*, photometry was

carried out in all *UVOT* bands through 7.5 kpc diameter apertures centred on the optical positions of red sequence galaxies. When combined with *GALEX FUV* and *NUV*, this creates essentially contiguous coverage of the entire ultraviolet region of the spectrum between $\sim$1000 and $\sim$3000 Å.

3 RESULTS

3.1 The UV upturn in Coma, Fornax, and Perseus

To analyse and compare the UV upturn in Coma, Fornax, and Perseus clusters, we plot the $FUV − V$ colour, the standard measure for the strength of the UV upturn, in fixed 7.5 kpc diameter apertures of all the cluster red sequence galaxies against their absolute *V*-band magnitudes as shown in Fig. 2. The brightest giant ellipticals tend to have the bluest colours and as such the strongest upturn. This is (as we will show) because they have hotter and more prominent extended HBs. We see a general trend of the $FUV − V$ colour getting redder with decreasing luminosity (mass). At $M_v \gtrsim −18$, however, as seen in Fornax galaxies, the $FUV − V$ trend with *V* is reversed and becomes bluer with decreasing luminosity. Obviously, the lack of systems with comparatively red $FUV − V$ colours at these magnitudes is simply a reflection of the *FUV* magnitude limit. However, the presence of galaxies with colours significantly bluer than $FUV − V < 5.5$ indicates that a significant fraction of the fainter dwarfs either have ongoing star formation or a UV upturn population with different characteristics to those of the more luminous galaxies, perhaps unsurprising given the mass and overall metallicity for these galaxies.

So far, these observations confirm the conventional view of the upturn as shown in Burstein et al. (1988) and Bureau et al. (2011). Note that the data for Perseus are subject to a comparatively large and therefore less certain Galactic extinction correction, and as a consequence, there may be an uncertain offset in the $FUV − V$ colours between Perseus and the other clusters. However, the range in $FUV − V$ colours is largely unaffected by this and is consistent with that found in the Coma and Fornax clusters (Virgo, Boselli et al. 2005).

Focusing only on the giant ellipticals, i.e. galaxies with $M_v \lesssim −18$, even with the brightest (most massive) galaxies tending to be somewhat bluer than their fainter counterparts, there is still significant stochastic variation of $1.5 \sim 2$ mag in range in the $FUV − V$ colour between the majority of galaxies in all three clusters, ignoring the few outliers. Where they have bands in common, the

photometric behaviour for each of the cluster populations appears consistent to the fidelity of the data, indicating that our results are most likely applicable to the general population of quiescent cluster early-type galaxies in the local Universe. However, this can only be verified with future studies involving larger sample of low-redshift clusters (Ali et al. in preparation).

The photometric range in UV-optical colour observed here agrees with that seen in the results of Boselli et al. (2005), who also found approximately 2 mag of scatter in the $FUV - V$ colour in red sequence Virgo cluster galaxies. As such the variation in the UV upturn strength appears to be a ubiquitous feature present in all low-redshift early-type cluster galaxies. This may be interpreted as a variation in the temperature and/or strength of an extended blue HB component in these galaxies.

If the blue colours at fainter magnitudes are due to an extended HB population in fainter galaxies rather than star formation, these may be relatively low-metallicity stars. In this case, the observed trend of $FUV - V$ becoming bluer with decreasing luminosity could simply reflect the lower mean metal abundance of the stellar population of dwarf galaxies (i.e. the conventional first parameter of HB morphology).

3.2 The UV SEDs of Coma galaxies

To properly investigate the nature of the sources of the UV upturn, we would need detailed UV spectra of the galaxies in question, data that are not available at present. The broad consensus is that the UV flux is produced by hot HB stars. Brown et al. (1997) obtained UV spectra of some bright galaxies from Ultraviolet Imaging Telescope (UIT) and found their temperatures to be consistent with a hot HB with $T_{\rm eff} \sim 20\,000$K. Imaging of the resolved sources of the UV upturn in M31 and M32 (Brown et al. 1998) confirms their nature as stars in the extended HB.

We have used the *GALEX* and UVOT data for the Coma cluster to build a detailed SED for red-sequence galaxies within the UVOT and *GALEX* images, covering between 1000 and 3000 Å uniformly for these objects. From *GALEX*, we use data from both the *FUV* and *NUV* bands, and from UVOT, we use data from the *UVW*2 and *UVW*1 to give us a contiguous coverage in the UV. We also make use of the UVOT *U*, *B*, and *V* data to give us coverage in the optical all the way up to approximately 6000 Å. We plot all colours relative to *V* in Fig. 3.

We detected 176 confirmed early-type cluster members in the *GALEX* bands as shown in Fig. 2, i.e. all Coma galaxies brighter than $M_v \leq -18$ in the region covered by *GALEX*. Of these, 44 were also targeted in UVOT pointings and all were detected. We then made a cut at $U - V = 2.1$ (this was done in addition to the $g - r$ red-sequence selection), and all galaxies with colours bluer than this limit were rejected in order to ensure that no systems with significant residual star formation were included. This left us with the 42 galaxies altogether, as shown in Fig. 3 (both red and cyan points in the plot combined).

We also plot the SED of IC4040, a known star-forming galaxy within Coma, and the SED of a 'red and dead' galaxy as given by the Conroy, Gunn & White (2009) (C09 henceforth) model, as these two SEDs represent the extreme cases of strong ongoing star formation and no star formation at all to compare with our sample of red-sequence galaxies. As one would expect, the spectrum of IC4040 is much flatter going from the optical to the ultraviolet when compared to the red-sequence galaxies. This is due to the initial mass function (IMF) of a star-forming system producing stars of a range of temperatures from faint M types all the way to
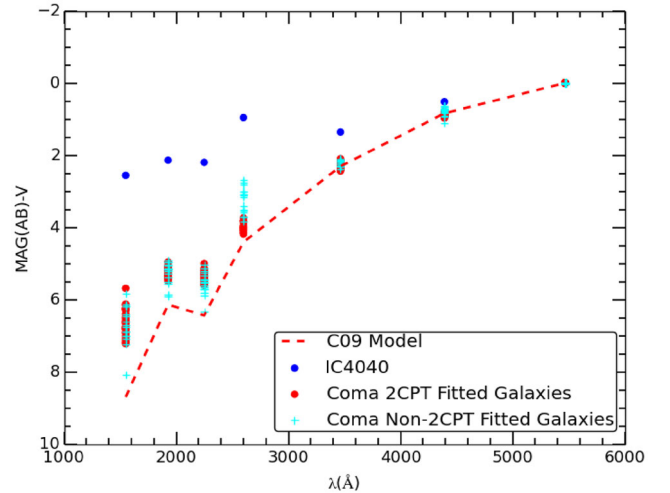

Figure 3. UV to optical SEDs of Coma red-sequence galaxies, IC4040 (a star-forming galaxy) and an old metal-rich SSP (no star formation) from the C09 model. The colours plotted (from left to right) are $FUV - V$, $UVW2 - V$, $NUV - V$, $UVW1 - V$, $U - V$, and $B - V$. Photometric error in colour is $\lesssim$ 0.1 mag.

OB supergiants, which emit strongly at all wavelengths between optical and ultraviolet, leading to a flat spectrum. Compared to this, the upturn galaxies have a bimodal population, consisting of a majority of low-temperature stars (mostly K giants by luminosity) superimposed with a relatively small but very hot sub-population of (likely) blue/extreme HB stars.

Unlike optical colours, the UV colours show considerable scatter. This is due to the different strengths, and temperatures (as we shall see) of the hot HB component. While the scatter increases towards bluer colours, as we would assume, we also find that, unexpectedly, there is large scatter in the $UVW1$ (2600 Å)$-V$ colours, even though this filter is the reddest of the UV filters we use. We will discuss this further when fitting blackbody curves to the UV SEDs.

3.2.1 Blackbody fitting

We now attempt to model the observed SEDs. We assume that the galaxies consist of a conventional old stellar population (with no attempt to model a hot post-MS phase) plus a secondary hot HB component. For the old SED, we choose a standard quiescent stellar population from C09, with solar metallicity and a formation redshift of $z_f = 4$ (low-redshift UV-optical colours change very little between $z_f = 3$ and $z_f = 6$ in these models). This is found to reproduce the optical colours of early-type galaxies well and produces 'normal' very red UV colours ($FUV - V \sim 8.5$) that are consistent with the expectations of conventional stellar evolution models. Importantly, this SED matches the UV colours of 47 Tucanae, (Dalessandro et al. 2012) and other metal-rich globular clusters as well as the reddest (but un-reddened) early-type galaxies with an HB nearly all confined to the red clump and with only a minor contribution from secondary populations with small He spreads. These are all old systems but do not have UV upturns.

We then model the hot HB with a single blackbody (of a given temperature) plus variable extinction following the Milky Way law (Cardelli, Clayton & Mathis 1988), to fit the UV SED of Coma early-type galaxies. We minimize least squares to fit the UV SEDs over a grid of reasonable values for temperature and extinction. It

is important to note that the fitting is carried out in the UV part of the spectrum (i.e. *GALEX FUV*, UVOT *UVW*2, *GALEX NUV*, UVOT *UVW*1), since it is most affected by the upturn. Nevertheless, we add the contribution of this component to the SED of the old stellar population at every wavelength considered through to the *V* band. In any event, the actual contribution longwards of 3000 Å is negligible. This works under the assumption that the spread in optical colours is small, and the base C09 model chosen reflects the observed optical colours very well, which can be seen to be the case in Fig. 3. Furthermore, the interstellar extinction in these galaxies would also need to be very small and we find this to be the case just from fitting to the UV part of the spectrum (see later).

Of the 42 total galaxies, we obtained very good fits to a single temperature blackbody (which we interpret as the mean blue HB star temperature) for 26 galaxies, from which we also derive a value for the interstellar extinction, which was generally low (*Av* $\lesssim 0.2$). However, some galaxies appear to show excess flux in the *UVW*1 filter (2600 Å), such that it is not possible to obtain a good fit (especially given the small number of points). These sources are represented by the SED points plotted in cyan in Fig. 3; clearly the spread in the 2600 Å photometry is much wider than that for the other UV points. We have checked the date of observations and find no correlation with those galaxies, giving a poor fit. The objects that are clearly discrepant in the *UVW*1 − *V* colour are randomly distributed in all other colours. It simply appears that there is anomalous behaviour in the *UVW*1 band for a subset of these galaxies.

The galaxies with a poor fit to our models are rejected based on a least-squares criterion. The distribution of this value across the sample is strongly bimodal (i.e. the good fits are fitted very well while the bad fits are significantly and clearly worse). The majority of poorly fit galaxies have very blue *UVW*1 − *V* colours. So although we do not do this, had we chosen to make a colour cut at approximately *UVW*1 − *V* = 3.8 (see Fig. 3) and a priori rejected all galaxies with a bluer colour, we would have rejected the majority of our poorly fit galaxies purely on this criterion.

The discrepant objects are largely (but not exclusively) found in a single UVOT *UVW*1 image (PSNJ13003230+2758411) that contains a few galaxies with a good fit. This may point to systematic problems with this particular image, though the fact that good fits were obtained with it and bad fits also occurred elsewhere means we cannot be certain about this.

We note from Fig. 4 that IC4040 also shows a comparatively high flux in this band, perhaps indicating that this may be a signature of residual star formation dominating in the UV. To explore this, we created composite SEDs from a C09 model supplemented with a scaled version of the IC4040 SED to generate SEDs with star formation that acted to increase the *U*-band flux of the simulated SED by 1–20 per cent above that of the C09 value. Given the tightness of the range (∼0.1 mag) in *U* − *V* colours of our selected objects, the models with up to a 10 per cent increase in *U*-band flux were plausible fits to our *optical* data. We then looked at the UV part of these simulated SEDs. Only the model with the smallest component of star formation (1 per cent) gave a plausible fit with the C09 plus BB model, even then it is far redder in UV-optical colours than all of our well-fitted galaxies – the star-forming component only increases the UV brightness relative to C09 alone by a few tenths in magnitude. All others fail largely because of their *NUV* − *UVW*1 colour being too steep for any C09 plus BB model. Consequently, from this exercise it is clear that star formation models do not generate the UV upturns we see in the galaxies with good fits. Any one colour could be fit, but not the entire UV-optical SED.

Table 1. The derived parameters (Blackbody temperature, Av, Normalization) from model fitting as shown in Fig. 4. The 'Normalization' parameter gives the relative percentage normalization of the black bodies to the base C09 model at the *GALEX* NUV band (i.e. 100 per cent indicates that the blackbody flux is equal to the C09 flux at this wavelength.)

Name	Mr	BB Temp	Av	Normalization (NUV)
NGC4889	−23.48	21 000	0	340
D80.106	−19.82	13 000	0	468
NGC4867	−21.14	15 000	0	374
NGC4874	−23.05	19 000	0	216
D80.153	−20.00	15 000	0	340
IC3976	−20.59	15 000	0.2	478
NGC4875	−20.47	16 000	0	287
IC3973	−21.00	15 000	0	298
D80.125	−19.75	14 000	0	322
NGC4869	−21.48	15 000	0	255
NGC4873	−20.95	12 000	0.1	454
NGC4876	−20.82	15 000	0	236
D80.132	−19.71	13 000	0	278
IC3968	−19.78	13 000	0	268
NGC4871	−21.17	15 000	0	204
D80.123	−19.97	10 000	0.1	500
IC3998	−20.52	15 000	0	198
NGC4883	−20.96	14 000	0	215
D80.127	−19.32	12 000	0	291
D80.154	−19.53	10 000	0.1	448
NGC4872	−20.89	13 000	0	210
D80.156	−19.34	12 000	0	238
D80.107	−19.87	10 000	0	351
D80.101	−20.19	12 000	0	220
D80.126	−19.61	10 000	0	349
D80.128	−19.66	10 000	0	307

We also attempted to fit the SEDs of our poorly fit (C09+BB) galaxies with the C09+RSF models, but fail to get good fits to their SEDs. However, we cannot rule out the possibility that this subset of galaxies has UV emission due to some residual star formation that could be accounted for by a more sophisticated residual star-forming (or upturn+RSF) models.

Furthermore, we also note that *HST* WFC3/F336W imaging data for red-sequence galaxies in Abell 1689 (which is close to rest frame ∼2600 Å) do not show the abnormally large spread in equivalent colour as seen in the UVOT data for Coma (Ali et al. in preparation), indicating that this is likely an issue with some of the *UVW*1 data and not a genuine feature of some UV SEDs. As we cannot explain this discrepancy and it appears to be a problem with a subset of a single band's photometry, we exclude the affected objects from further discussion.

There is no intrinsic reason why the best blackbody fits could not contribute significant flux in the optical bands because the fit is not constrained there. The fact that the blackbody fits never do this strongly supports the idea that the UV is dominated by the component modelled here as a blackbody, while the optical is completely dominated by the conventional old metal-rich stellar population. As a consistency check, we have performed the entire model fitting process for the whole spectrum (UV and optical points), allowing both blackbody and C09 components to vary across the wavelength range and find that although there are some minor changes to the individual results obtained for each galaxy, the overall trends and conclusions remain intact.

All major derived parameters for the good fit galaxies are given in Table 1. Fig. 4 shows the galaxies with their corresponding best-fitting models. In the first panel, we also show the underlying C09
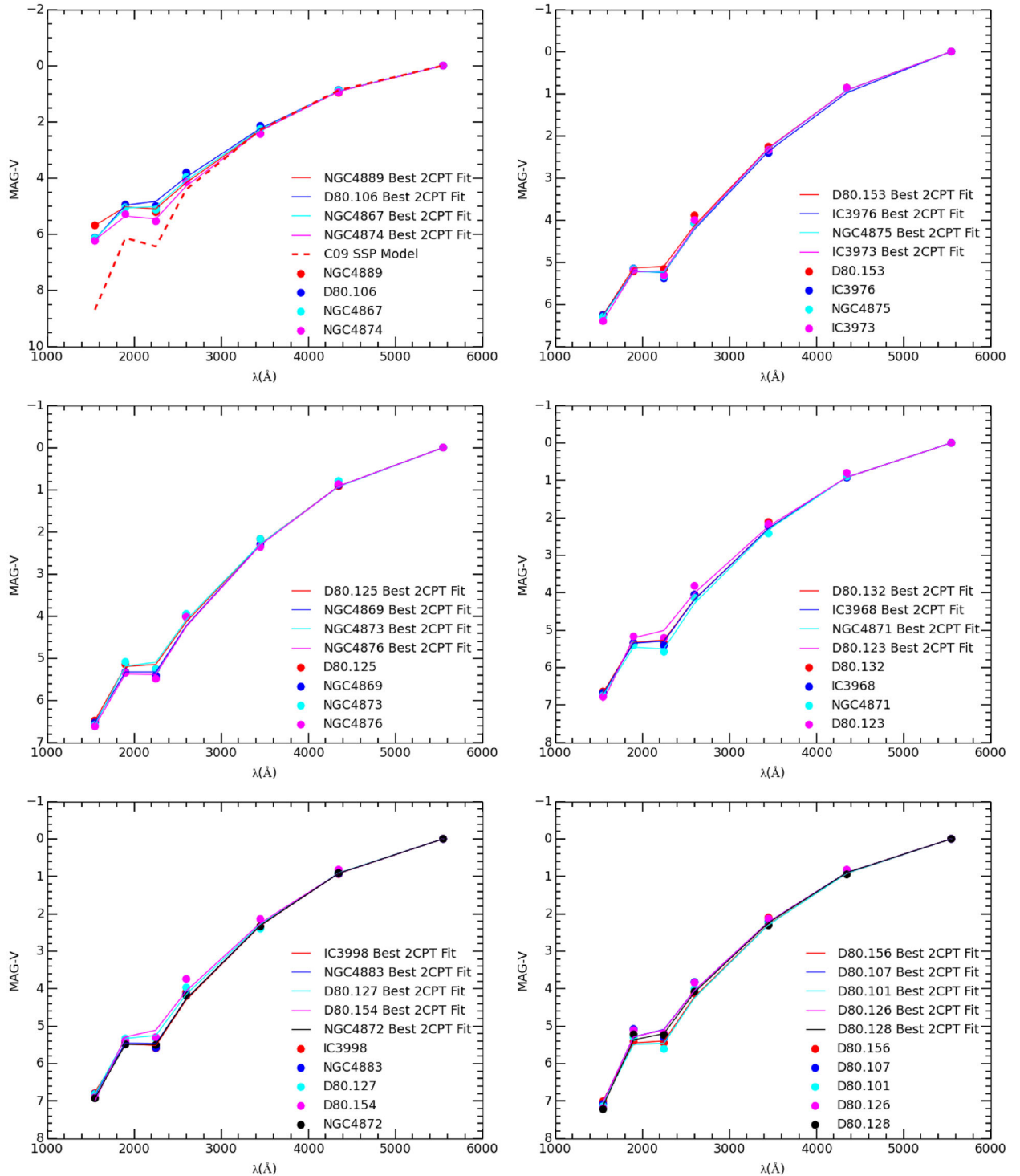
Figure 4. UV to optical SEDs of 26 Coma red-sequence galaxies that were well fitted with two component (C09 + Blackbody) models. Galaxies are identified in the figure caption, by their NGC/IC numbers or their number in Dressler (1980)'s catalogue. Once again, the colours plotted (from left to right) are $FUV - V$, $UVW2 - V$, $NUV - V$, $UVW1 - V$, $U - V$, and $B - V$. Photometric error in colour is $\lesssim 0.1$ mag. The dashed red line in the first panel indicates the baseline SED derived from Conroy et al. (2009) upon which the blackbody component is added to fit the individual galaxy SEDs.

model showing the contribution of the purely old population, clearly demonstrating that the extra blackbody component only contributes to the UV part of the SED. The fitted blackbody component usually has a temperature between 10 000 and ∼21 000 K, consistent with the earlier UIT observations of Brown et al. (1997) and the indices

derived by Le Cras et al. (2016) for massive BOSS galaxies. We plot the derived temperature versus M_r (a good proxy for stellar mass) in Fig. 5 and we find a strong correlation between temperature and mass (and therefore metal abundance), in the sense that more massive (and metal-rich) galaxies have hotter (and stronger)
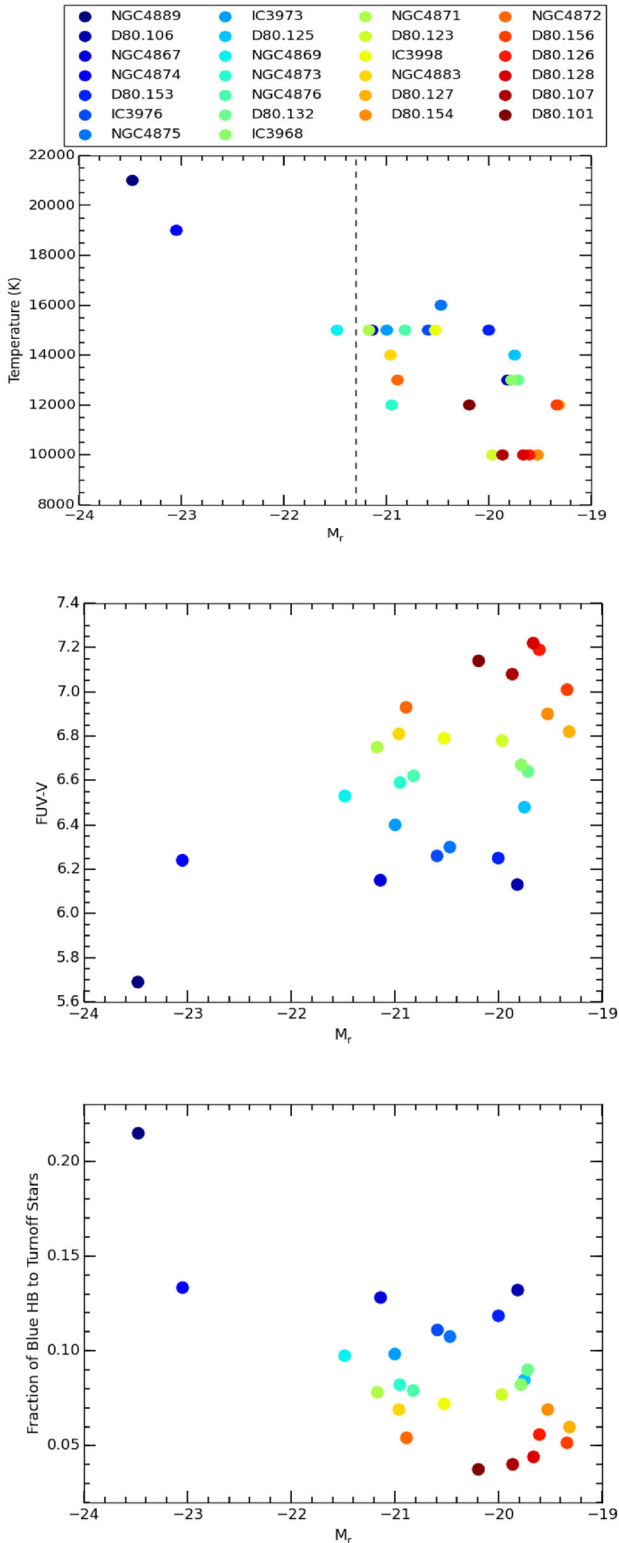
NGC4889	IC3973	NGC4871	NGC4872
D80.106	D80.125	D80.123	D80.156
NGC4867	NGC4869	IC3998	D80.126
NGC4874	NGC4873	NGC4883	D80.128
D80.153	NGC4876	D80.127	D80.107
IC3976	D80.132	D80.154	D80.101
NGC4875	IC3968		

Figure 5. Top: The best-fitting blackbody temperature versus M_r for galaxies in Coma. There is a clear trend of higher T_{eff} with increasing luminosity (and hence increasing mass and metallicity). Dashed line shows M^* for Coma (Eisenhardt et al. 2007). Typical errors in temperature are of the order ± 1000 K, the quantisation we use in our fitting process. Middle: this shows $FUV - V$ versus M_r for these same galaxies, showing how the increasing temperature drives the bluer colours. Photometric error in colour is $\lesssim$ 0.1 mag. Bottom: The estimate of the ratio of blue HB stars to turn-off stars within each galaxy as a function of M_r for these objects.

HB components. This also recovers the $FUV - V$ versus V anti-correlation, as observed by Burstein et al. (1988) and Bureau et al. (2011). We note here that since the hot component does not have a single temperature for all galaxies, one cannot use a single UV-optical colour, e.g. $FUV - V$ to measure the upturn in a uniform manner and classify sources as in Yi et al. (2005, 2011), a point also made by Smith et al. (2012).

Nelan et al. (2005) and Thomas et al. (2005, 2010) demonstrated through a spectroscopic analysis that both metallicity and age were correlated with the velocity dispersion and therefore mass of early types with Price et al. (2011), demonstrating similar behaviour in Coma early types. The variation in the $FUV - V$ colour of the C09 models with age beyond 8 Gyr does not change their contribution to the UV spectrum, therefore validating our decision to use a single-age model for all of our fits to the optical photometry regardless of the luminosity. Similarly, for our $g - r$ selection, metallicity is expected to vary between $1 - 2Z_\odot$. However, as a test of consistency, we duplicated out fitting procedure using a C09 model with $Z = 0.56Z_\odot$, in particular to check whether such a sub-solar model yields a better fit for the lowest luminosity galaxies in our sample. We find that for all such galaxies, using a base sub-solar metallicity model gives worse fits to the optical colours than using a solar metallicity model. Furthermore, the most reasonable fits of the sub-solar metallicity models required very large values of interstellar extinction ($A_v \sim 0.7$), which are clearly unphysical for these systems. Conversely, for the most luminous galaxies in our sample – which are likely to be of supersolar metallicity – a base solar metallicity C09 model is already overestimating the contribution from the underlying conventional stellar population, given that the supersolar metallicity models have redder UV-optical colours.

To test the effect of a supersolar metallicity model, we repeated our entire fitting procedure using a base C09 Simple Stellar Population (SSP) with $Z = 1.78Z_\odot$ (the next highest Z available after $Z = Z_\odot$), likely to be appropriate for the top 50 per cent of the brightest galaxies in our sample. We find that the best-fitting temperatures decreased by on average ~ 1000 K, but the blackbody normalizations increased significantly between ~ 200 and 500 per cent to compensate for the combination of a decrease in blackbody temperature and the underlying supersolar SSP being redder in the UV. However, despite the change in temperatures and normalizations when using a base supersolar metallicity model, the overall trend seen in Fig. 5 (top) still remained intact.

Given the high metallicity and old ages (and therefore the restricted range of both) for the conventional stellar populations in all of these galaxies, neither their metallicity nor age can therefore be driving the correlations seen in Fig. 5. Note that we are not saying that there is no correlation between overall age and strength of UV upturn in the actual systems. We are merely stating that the C09 models include no component that specifically attempts to replicate anything that may give rise to a UV upturn, unlike e.g. the Yi et al. (1999) models. The parameters of the blackbody components that we use to fit the upturn may correlate with overall age, but we do not attempt to make this explicit.

4 DISCUSSION

4.1 Hot HB stars as the source of the UV upturn

We have measured vacuum UV colours and the UV SEDs for quiescent early-type galaxies in three low-redshift clusters, reaching to the L^* point and somewhat beyond. Across this entire luminosity (mass) range, we find evidence for a UV-bright stellar population

that we relate to the classical upturn (O'Connell 1999). Reflecting the scatter in $FUV - V$, all of the galaxies undergoing our fitting procedure require an extra blackbody component on top of the C09 SED model to account for their UV SED. Moreover, the temperature of this component seems to increase with optical luminosity, albeit with some scatter. The need for this component is already clear in the scatter of $FUV - V$ colour in the absence of similar scatter in the optical colours.

Residual star formation does not produce an SED consistent with our observations (cf. our discussion of IC4040 above). The most likely source of the excess UV flux is a hot HB component, as earlier argued by Greggio & Renzini (1990), Brown et al. (1997), and O'Connell (1999). While blue HBs are commonly observed in metal-poor star clusters, it is very unlikely that our observations can be explained in this fashion. Our galaxies are largely metal rich and their HB should largely coincide with the red clump at temperatures of around 4000–5000 K: too cool to provide the observed UV emission in the upturn galaxies. Given the small fraction of the lifetime that stars live on the HB, it would require a significant low-metallicity main-sequence population to exist within these galaxies, which is explicitly ruled out by many studies determining the metallicities of such galaxies. The explanation of these UV upturn galaxies lies in the understanding gleaned from observations of the resolved stellar populations in high-metallicity open clusters and so-called second parameter globular clusters (Catelan 2009; Peacock et al. 2017).

The most likely mechanism to explain the presence of hot HB stars in comparatively metal-rich systems (by globular cluster standards, i.e. where the HB should not extend beyond the RR Lyra gap according to canonical models) involves Helium enrichment. In Milky Way globular clusters such as ω Centauri and NGC2808, multiple main sequences are found to correspond with multimodal blue HBs and spectroscopic evidence shows that the bluer stars are more metal rich than the red ones (Piotto et al. 2005, 2007; Bragaglia et al. 2010). The only way for this to be possible is for the bluer stellar population to be enriched in Helium relative to the redder population. There is indirect evidence of this in the selective abundance patterns of the proton-capture elements, which indicates processing through the Mg-Al chains during hot bottom burning, a process that may also dredge up Helium to the surfaces (e.g. see Gratton, Carretta & Bragaglia 2012 and Charbonnel 2016 for reviews). The He abundance may be as high as $Y = 0.43$ for the most extreme population in NGC2808 (Milone et al. 2015). In other words, the anomalously hot HB stars in Galactic globular clusters arise from a population with significantly enhanced Helium abundance.

Some of the more metal-rich globular clusters in the bulge, such as NGC6388 and NGC6441 (which have [Fe/H] $\sim - 0.5$, at the high-metallicity tail of the distribution in the Galaxy), also have extended HBs. Tailo et al. (2017) show that these stars have temperatures of up to 14 000 K for a Y of 0.38. A specific Galactic system that provides a possible model for a Helium-enriched high-metallicity and old population is the open cluster NGC6791 (cf. Dorman, O'Connell & Rood 1995 for a similar remark). In many ways, this resembles a miniature version of elliptical galaxies. Buzzoni et al. (2012) demonstrate that it has a single stellar population with an age of 9 Gyr and [Fe/H] of $+0.3$. It is also considerably α-element enhanced and has $Y = 0.30 \pm 0.04$ (Linden et al. 2017, though see Boesgaard, Lum & Deliyannis 2015). Its HB contains a significant blue population and its integrated SED is essentially indistinguishable from strong UV upturn elliptical galaxies. Buzzoni et al. (2012) argue, given this similarity, that Helium-enriched

HB stars are therefore an extremely strong candidate to explain UV upturns in elliptical galaxies. Despite it being a single and possibly unusual object (but cf. Berkeley 17, Bragaglia et al. 2006), NGC6791 represents the *only* resolved stellar counterpart to the sources of the upturn in external galaxies and therefore remains the best heuristic model with which to interpret this UV excess in galaxies.

While He-enhanced HBs have been directly observed, there are other theoretical possibilities for producing a UV upturn population. These include scenarios where there is extra mass-loss in the RGB (Yi et al. 1999; Yaron, Kovetz & Prialnik 2008), possibly due to binary interactions (Han et al. 2007; Carraro & Benvenuto 2017). However, in this case, the degree of mass-loss or the close binary fraction would somehow (e.g. via metallicity, Yi et al. 1999) have to depend strongly on galaxy mass and neither explanation would account for the observations in globular clusters, where the blue HB segments are clearly related, by chemical tagging, to the multiple main sequences (Milone et al. 2015). This would be in contrast with recent observations by Badenes et al. (2017), where the binary fraction *decreases* with increasing metallicity, opposite to what would be needed to explain the observed trends. Moreover, there is no observational evidence for enhanced mass-loss on the RGB depending on metal abundance (e.g. see Miglio et al. 2012; Salaris, Cassisi & Pietrinferni 2016). In any event, most of the mass-loss would be expected to happen at the AGB, i.e. after the HB phase.

All this points to the presence of a He-rich sub-population in these galaxies producing hot HB stars at the end of their lifetime. Given that stars spend a small fraction of their lifetimes in the HB (~ 1 per cent), they represent a much larger number of He-enhanced stars within the galaxy.

4.2 Implications for galaxy formation

Given our blackbody fits to the UV upturns, we can then use UV photometry of individual hot HB stars in local globular and open clusters to provide estimates of the properties of the UV upturn populations. First, given the estimated temperature of our BB fit for a given galaxy, we can estimate a corresponding value of Y (since higher He abundance leads to hotter HB stars). Secondly, from the observed absolute luminosities of local hot HB stars (e.g. from Sweigart et al. 2002; Recio-Blanco et al. 2006), we can deduce the number of such stars needed to account for the galaxy's *FUV* output.

To relate this to a global population fraction, we adopt an HB lifetime of ~ 100 Myr and ~ 1 Gyr for stars to evolve from the main-sequence turn-off to the Helium flash. To estimate the fraction of blue HB stars (i.e. the He-rich population), via the IMF, we need to assume an age for the 'normal' and He-rich populations. As a guide to the age since formation to use for our stellar populations, we take the old, metal-rich open cluster NGC6791 as a suitable model. This requires a Helium-enhanced population with $Y = 0.34$ to explain its blue HB and consequent UV upturn, which is very similar in colour to those of our typical galaxies. We then use the YEPS spectrophotometric models for He-enhanced stellar populations (Chung et al. 2017), with $Y = 0.34$, to derive an age of 12 Gyr for these stars to match the observed UV colours and temperatures. That is, with this level of He enrichment, it takes ~ 12 Gyr for the upturn to become apparent in the YEPS models' simulated colours (see also Tantalo et al. 1996). We can therefore determine the relevant masses for the turn-off stars, etc., in order to calculate the relative numbers of HB and total stars from the IMF.

In fact, if we assume that both the He-enriched and 'normal' populations are formed in effectively simultaneous coeval bursts, we should expect that the main-sequence lifetimes of the He-rich population stars are shorter than those of the normal population (Chantereau, Charbonnel & Decressin 2015). Consequently, at any given time, the He-rich stars reaching the HB should be of lower mass than those of the other population. If we assume that HB luminosities are largely independent of mass (as observed in NGC2808; Piotto et al. 2007), then as time goes on, given a normal IMF, an increasing number of stars enter the blue HB. If this is not matched by a shorter HB lifetime, the overall UV luminosity contributed by the He-rich HB population will increase. Thus, our base estimate of the fraction of He-rich stars, from above, will be an *over*estimate.

However, we note that the YEPS He-enhanced SSP models imply a constant UV luminosity with time once a blue HB is formed, rather than one where the UV luminosity increases. This may be because, in their models, the time spent on the HB decreases with stellar mass, compensating for the increasing rate of stars entering the blue HB with time due to the slope of the IMF. If this is the case then we should expect our upper limits to be close to the real values.

A full treatment of this would require a detailed study of the relevant isochrones and is beyond the scope of this work. However, to progress we can make the (incorrect) assumption that the MS lifetimes of the two populations are the same (leading to the same mass stars joining the HB at the same time) and thereby determine an upper limit to the fraction of stars in the He-rich population for each of our galaxies. By then making an estimate of the correction to the relevant mass of the He-rich population and assuming a standard slope for the IMF, we can estimate a correction to this upper limit, thereby indicating whether the derived upper limits are likely to be close to the true values.

Given the above, we consider ages since formation of both stellar populations to be 12 Gyr. Not only is this consistent with the indication given by NGC6791, but it also agrees with spectrophotometric and spectroscopic measurements on early-type galaxies with masses similar to those used here, where red-sequence galaxies are found to evolve passively and with no increase in colour spread at least to $z \sim 2$, and probably higher, with quiescent galaxies observed to $z \sim 4$, including in the Dark Energy Survey data (C. Maraston, private communication) and elsewhere (e.g. Glazebrook et al. 2017). This points to high redshifts of star formation and no significant further episodes at later times (see also Thomas et al. 2010). Assuming these ages, we find that a range of between 4 and 20 per cent of stars in our sample galaxies evolve on to the blue HB. This is a similar fraction as that suggested by Dorman et al. (1995) and observed in some local stellar clusters (see below), and also as estimated by Le Cras et al. (2016) for massive BOSS galaxies. The fractions and temperatures of these stars appear to depend on the luminosities of their parent galaxies, suggesting that the origin of the hot HB population is related to the internal chemical evolution of galaxies.

Similar behaviour is seen in a minority of local globular and open clusters that have a wide spread in Helium abundances within their stellar populations (with NGC2808 and ω Centauri being the prime examples). In these cases, 10–30 per cent of stars seem to have $Y \sim 0.34$–0.40 (Piotto et al. 2007; Buzzoni et al. 2012; Tailo et al. 2017). Note that a significant fraction of the population may also be more He rich than the cosmological value but do not produce hot HB stars because of their high metallicities; this appears to be the case for the objects studied by Tailo et al. (2017), where two third of the stars may have $Y > 0.24$.

Individual HB stellar temperatures appear to correlate with Helium abundance, e.g. for NGC2808 $T_{\rm eff}$ of nearly 40 000 K for stars with $Y = 0.43$. Most of our galaxies are fitted with $T_{\rm eff} \sim 15\,000$ K indicating that any He-enhanced population within them have lower Y than this, similar to that of NGC6791. This allows us to assess any correction required to the fraction of stars in this He-enhanced population due to the assumption of equal stellar mass used in the estimation of the upper limit. In Chantereau et al. (2015), a $Y = 0.4$ star with $0.6\,\rm M_{\odot}$ has a main-sequence lifetime of 11.1 Gyr, compared to 11.9 Gyr for a $0.8\,\rm M_{\odot}$ counterpart with cosmological He abundance. If we assume that stars of these masses reach the HB at the same time, then for a typical IMF slope, this implies twice as many H-enriched stars than if we assumed (as above) that the MS lifetime was independent of Y. Consequently, assuming that the increased rate of entry on to the HB by He-enriched stars is not matched by a decrease in their HB lifetime *and* that HB luminosity does not vary overly with stellar mass, this difference implies that the true fraction of stars with enhanced He abundances should be within a factor of ~ 2 of our simple (upper limit) estimate. Given that all except the most massive of our galaxies are likely to have $Y < 0.4$, even this factor ~ 2 is likely to be itself an upper limit. One final *caveat* on this estimate is that even though we might expect a Y-related variation in turn-off mass and main-sequence lifetime, no difference in the MS turn-off mass has been reported for any of the stellar populations with varying Y in NGC2808 (Milone et al. 2015).

4.2.1 Effect on early evolution

Assuming that our blackbody component can be interpreted as a Helium-enhanced population, this population appears to be more enriched and more abundant as a function of galaxy mass. As galaxy mass and metallicity are, in general, thought to be correlated in early-type galaxies, this may suggest a relation between Y and Z, unsurprising given the predictions of many models of stellar nucleosynthesis. This suggests that these objects originate from the normal process of galaxy chemical evolution and are formed *in situ*. We know from Carter et al. (2011) that the hot HB component is centrally concentrated, as expected if the He enrichment comes from the same processes of chemical evolution. Given that our observations mirror those of Buzzoni et al. (2012), our results therefore imply a rapid enrichment for a large mass of stars *in situ*, and therefore rapid formation of massive haloes at high redshifts (in agreement with, e.g., Glazebrook et al. 2017; Jørgensen et al. 2017).

Using the same assumptions as those in Chung et al. (2017) and Buzzoni et al. (2012), if we take ~ 12 Gyr as a typical age for our stellar populations (as above) our data allow us to set a lower limit to the stellar mass of these galaxies at $z \sim 4$. Assuming 4–20 per cent of the stars to be sufficiently He rich to evolve to the hot HB (Fig. 5, bottom), an L^* galaxy must have a stellar mass of at least 0.3–$0.8 \times 10^{10}\,\rm M_{\odot}$ in place at $z \sim 4$ or earlier, with all the caveats noted above. This in turn implies that the bulk of the stellar population may be even older. Varying the assumed age of the stellar population by 2 Gyr only changes the fraction of He-rich stars by ~ 1.5 per cent. In any event, there needs to be an earlier population to produce the extra Helium. The only way this argument may be incorrect is if the Y value of this population is even more extreme, in which case the stars can reach the HB in a significantly shorter period of time. Given the abundance yields of any prior population that gives rise to the enhanced He fractions of the hot HB stars, it is likely that this earlier population must be an order of magnitude

more massive than the values estimated above (D'Antona et al. 2016). This would imply that nearly all of the stellar mass observed today in these galaxies is in place at high redshift. We note that even if our assumption of typical $Y \sim 0.34$ and therefore 12 Gyr as an age for stellar populations of our typical galaxies is incorrect, the lack of evidence for appreciable star formation at $z < 2$ (Jørgensen et al. 2017 find formation redshifts for cluster galaxies between $2 < z < 6$ depending on the diagnostics used) limits their age to >10 Gyr (requiring higher Y). Even then, similar arguments can be made as to how much stellar mass needs to be present by this time.

There have been alternative models invoked to explain an increased Helium abundance in galaxies, for example those involving Helium sedimentation in galaxy-cluster scale haloes (Peng & Nagai 2009). Here, we would note that our results seem to run counter to the predictions of Helium sedimentation. Our most massive galaxies appear to have the highest Helium enhancement and likely contain the oldest stellar populations. Helium sedimentation acts to increase the He enhancement with increasing time and over time-scales of billions of year.

If a helium-enhanced sub-population is not accounted for, it is possible that galaxy properties derived from photometry and spectroscopy may be misleading or misinterpreted. Interpretation of spectral indices, particularly those involving Balmer lines may be incorrect if the Helium abundance and the presence of a hot HB is not correctly accounted for (de Freitas Pacheco & Barbuy 1995; De Propris 2000; Percival & Salaris 2011) and so derived quantities such as ages and metallicities of old stellar populations might appear self-consistent, yet be inaccurate. The YEPS photometric models (Chung et al. 2017) show the required behaviour for late-time evolution, showing UV upturns, but imply that for reasonable metallicities, most broad-band optical colours are unaffected by varying He abundance over the range modelled at intermediate ages. However, stellar populations younger than 1 Gyr are not presented and so the effect on the colours of, e.g., Lyman break galaxies and other young systems is unclear.

5 CONCLUSIONS

We have shown that the UV upturn is a common phenomenon in quiescent early-type galaxies to luminosities well below the L^* point. All galaxies appear to show at least some fraction of a UV-bright population. Characterizing this upturn with a blackbody component, the temperature and mass of this population appear to vary with the mass (and therefore metallicity) of the galaxy, in the sense that brighter and more metal-rich systems have the hottest and more luminous UV fluxes. We interpret this, in common with other studies, as evidence for the presence of hot HB stars in these galaxies. This interpretation of our results indicates that the more massive galaxies have the most extreme HBs. An explanation of this consistent with the findings of local stellar populations (e.g. in star clusters) is that these stellar populations are systematically enriched in Helium. If this is the case, then, noting the caveats discussed in Section 4.2, we can estimate that up to 4–20 per cent of the turn-off stars (galaxy-dependent) must be so enriched as to evolve on to the blue HB, with Y of about 0.34 to explain the observations of our typical galaxies.

Interpreting our results via the recent YEPS stellar population synthesis models of Chung et al. (2017) implies that at least $\sim 0.5 \times 10^{10}$ M$_\odot$ from the He-enriched sub-population alone needs to be in place, certainly by $z = 2$ and by $z \sim 4$ if our assumption of $Y \sim 0.34$ is reasonable. This interpretation implies that there is an upper limit to the redshift at which upturns are easily detectable,

given the main-sequence lifetimes of the He-enriched stars that go on to become hot HB stars. This limit may itself be dependent on galaxy mass through the correlation between this quantity and the current-day UV upturn properties. We will explore this in future papers.

REFERENCES

Alam S., et al., 2015, ApJS, 219, 12
Badenes C., Mazzola C. et al., 2017, preprint (arXiv:1711.00660)
Bertola F., Capaccioli M., Oke J. B., 1982, ApJ, 254, 494
Boesgaard A. M., Lum M. G., Deliyannis C. P., 2015, ApJ, 799, 202
Boselli A. et al., 2005, ApJ, 629, L29
Bower R. G., Lucey J. R., Ellis R. S., 1992, MNRAS, 254, 601
Bragaglia A., Tosi M., Andreuzzi G., Marconi G., 2006, MNRAS, 368, 1971
Bragaglia A. et al., 2010, ApJ, 720, L41
Brown T. M., Ferguson H. C., Davidsen A. F., Dorman B., 1997, ApJ, 482, 685
Brown T. M., Ferguson H. C., Stanford S. A., Deharveng J.-M., 1998, ApJ, 504, 113
Brown P. J., Breeveld A. A., Holland S., Kuin P., Pritchard T., 2014, Ap&SS, 354, 89
Brunzendorf J., Meusinger H., 1999, A&AS, 139, 141
Bureau M. et al., 2011, MNRAS, 414, 1887
Burstein D., Bertola F., Buson L. M., Faber S. M., Lauer T. R., 1988, ApJ, 328, 440
Buzzoni A., Bertone E., Carraro G., Buson L., 2012, ApJ, 749, 35
Cardelli J. A., Clayton G. C., Mathis J. S., 1988, ApJ, 329, L33
Carraro G., Benvenuto O. G., 2017, ApJ, 841, L10
Carter D., Pass S., Kennedy J., Karick A. M., Smith R. J., 2011, MNRAS, 414, 3410
Catelan M., 2009, Astrophys. Space Sci. Proc., 7, 175
Chantereau W., Charbonnel C., Decressin T., 2015, A&A, 578, A117
Charbonnel C., 2016, in Moraux E., Lebreton Y., Charbonnel C., eds, EAS Publ. Ser. Vol. 80. EDP Sciences, France, p. 177
Chung C., Yoon S.-J., Lee Y.-W., 2017, ApJ, 842, 91
Code A. D., 1969, PASP, 81, 475
Conroy C., Gunn J. E., White M., 2009, ApJ, 699, 486(C09)
D'Antona F., Vesperini E., D'Ercole A., Ventura P., Milone A. P., Marino A. F., Tailo M., 2016, MNRAS, 458, 2122
Dalessandro E., Schiavon R. P., Rood R. T., Ferraro F. R., Sohn S. T., Lanzoni B., O'Connell R. W., 2012, AJ, 144, 126
de Freitas Pacheco J. A., Barbuy B., 1995, A&A, 302, 718
De Propris R., 2000, MNRAS, 316, L9
Dorman B., O'Connell R. W., Rood R. T., 1995, ApJ, 442, 105
Dressler A., 1980, ApJS, 42, 565
Drinkwater M. J. et al., 2000, A&A, 355, 900

Eisenhardt P. R., De Propris R., Gonzalez A. H., Stanford S. A., Wang M., Dickinson M., 2007, ApJS, 169, 225

Ferguson H. C., Sandage A., 1988, AJ, 96, 1520

Gil de Paz A., et al. , 2007, ApJS, 173, 185

Glazebrook K., et al., 2017, Nature, 544, 71

Gratton R. G., Carretta E., Bragaglia A., 2012, A&A Rev., 20, 50

Greggio L., Renzini A., 1990, ApJ, 364, 35

Hammer D., Hornschemeier A. E., Mobasher B., Miller N., Smith R., Arnouts S., Milliard B., Jenkins L., 2010a, ApJS, 190, 43

Hammer D. et al., 2010b, ApJS, 191, 143

Han Z., Podsiadlowski P., Lynas-Gray A. E., 2007, MNRAS, 380, 1098

Jester S. et al., 2005, AJ, 130, 873

Jørgensen I., Chiboucas K., Berkson E., Smith O., Takamiya M., Villaume A., 2017, AJ, 154, 251

Karick A. M., Drinkwater M. J., Gregg M. D., 2003, MNRAS, 344, 188

Le Cras C., Maraston C., Thomas D., York D. G., 2016, MNRAS, 461, 766

Lee Y. -W. et al., 2005a, ApJ, 621, L57

Lee Y. -W. et al., 2005b, ApJ, 619, L103

Linden S. T. et al., 2017, ApJ, 842, 49

Markwardt C. B., Tueller J., Skinner G. K., Gehrels N., Barthelmy S. D., Mushotzky R. F., 2005, ApJ, 633, L77

Martin D. C. et al., 2005, ApJ, 619, L1

Michard R., Andreon S., 2008, A&A, 490, 923

Miglio A. et al., 2012, MNRAS, 419, 2077

Milone A. P. et al., 2015, ApJ, 808, 51

Morrissey P. et al., 2007, ApJS, 173, 682

Nelan J. E., Smith R. J., Hudson M. J., Wegner G. A., Lucey J. R., Moore S. A. W., Quinney S. J., Suntzeff N. B., 2005, ApJ, 632, 137

Norris J. E., 2004, ApJ, 612, L25

O'Connell R. W., 1999, ARA&A, 37, 603

O'Connell R. W., Rosario D. J., Schiavon R. P., Conselice C. J., Gallagher J. S., Wyse R. F. G., 2005, in Bulletin of the American Astronomical Society, Vol. 37, American Astronomical Society Meeting Abstracts, 1450

Pastorello N., Forbes D. A., Foster C., Brodie J. P., Usher C., Romanowsky A. J., Strader J., Arnold J. A., 2014, MNRAS, 442, 1003

Peacock M. B., Zepf S. E., Kundu A., Chael J., 2017, MNRAS, 464, 713

Peng F., Nagai D., 2009, ApJ, 705, L58

Percival S. M., Salaris M., 2011, MNRAS, 412, 2445

Piotto G. et al., 2005, ApJ, 621, 777

Piotto G. et al., 2007, ApJ, 661, L53

Poole T. S. et al., 2008, MNRAS, 383, 627

Price J., Phillipps S., Huxor A., Smith R. J., Lucey J. R., 2011, MNRAS, 411, 2558

Recio-Blanco A., Aparicio A., Piotto G., de Angeli F., Djorgovski S. G., 2006, A&A, 452, 875

Roming P. W. A. et al., 2005, Space Sci. Rev., 120, 95

Salaris M., Cassisi S., Pietrinferni A., 2016, A&A, 590, A64

Schlafly E. F., Finkbeiner D. P., 2011, ApJ, 737, 103

Schombert J. M., 2016, AJ, 152, 214

Smith R. J., Lucey J. R., Carter D., 2012, MNRAS, 421, 2982

Sweigart A. V., Brown T. M., Lanz T., Landsman W. B., Hubeny I., 2002, in van Leeuwen F., Hughes J. D., Piotto G., eds, ASP Conf. Ser. Vol. 265, Omega Centauri, A Unique Window into Astrophysics. Astron. Soc. Pac., San Francisco, p. 261

Tailo M. et al., 2017, MNRAS, 465, 1046

Tantalo R., Chiosi C., Bressan A., Fagotto F., 1996, A&A, 311, 361

Thomas D., Maraston C., Bender R., Mendes de Oliveira C., 2005, ApJ, 621, 673

Thomas D., Maraston C., Schawinski K., Sarzi M., Silk J., 2010, MNRAS, 404, 1775

Yaron O., Kovetz A., Prialnik D., 2008, in Deng L., Chan K. L., eds, Proc. IAU Symp. 252, The Art of Modelling Stars in the 21st Century. Cambridge Univ. Press, Cambridge, p. 261

Yi S. K., 2008, in Heber U., Jeffery C. S., Napiwotzki R., eds, ASP Conf. Ser. Vol. 392, Hot Subdwarf Stars and Related Objects. Astron. Soc. Pac., San Francisco, p. 3

Yi S., Demarque P., Oemler A., Jr, 1997, ApJ, 486, 201

Yi S., Lee Y., -W., Woo J., -H., Park J.-H., Demarque P., Oemler A., Jr, 1999, ApJ, 513, 128

Yi S. K. et al., 2005, ApJ, 619, L111

Yi S. K., Lee J., Sheen Y., -K., Jeong H., Suh H., Oh K., 2011, ApJS, 195, 22

York D. G. et al., 2000, AJ, 120, 1579

This paper has been typeset from a TeX/LaTeX file prepared by the author.